Applied Thermal Engineering 73 (2014) 914–923

Contents lists available at ScienceDirect

Applied Thermal Engineering

journal homepage: www.elsevier.com/locate/apthermeng

# Modeling and process simulation of controlled microwave heating of foods by using of the resonance phenomenon

Laura Analía Campañone [a, c, *], José Alberto Bava [b], Rodolfo Horacio Mascheroni [a, c]

[a] Departamento de Ingeniería Química, Facultad de Ingeniería, Universidad Nacional de La Plata, La Plata 1900, Argentina
[b] Departamento de Ingeniería Electrónica, Facultad de Ingeniería, Universidad Nacional de La Plata, La Plata 1900, Argentina
[c] CIDCA Centro de Investigación y Desarrollo en Criotecnología de Alimentos, (CONICET La Plata-UNLP). 47 y 116, 1900 La Plata, Argentina

## HIGHLIGHTS

- Resonance was applied to improve the uniformity of internal temperature.
- 3D mathematical model was developed, by solving the energy transfer.
- Maxwell equations were solved using Comsol Multiphysics software.
- The numerical predictions allow to develop strategically internal patterns.
- More uniformity of the final temperature profiles was achieved.

## ARTICLE INFO

*Article history:*
Received 24 February 2014
Accepted 21 August 2014
Available online 30 August 2014

*Keywords:*
Microwave heating
Uniformity
Wave interference
FEM

## ABSTRACT

Experimental and theoretical analyses of the controlled heating of foods were done. The purpose of this paper is to demonstrate the favorable effects of the use of the phenomenon of resonance to improve the uniformity of internal temperature profiles in foods during microwave heating. Particularly, the effect of the changing the phases of two opposite electric field excitations and their interaction with food samples was focused. With this aim, a 3D mathematical model was developed, by solving the energy transfer balance during the microwave heating process. It permits to analyze the resonance phenomena by predicting the electromagnetic energy distribution outside and its value inside the foods through the solution of Maxwell equations. The mathematical model was employed to simulate temperature data obtained from prototype. The numerical predictions allow strategically develop internal patterns of heating altering the phases of the incident waves, that enable achieve greater uniformity of the final temperature profiles.



## 1. Introduction

Microwave heating of foods is an efficient method capable of generating energy inside the product through the interaction of radiation, mainly with water molecules. Microwaves are applied to different processes showing some advantages such as reduction of the environmental impact, energy saving compared to conventional methods, use of clean energy, spatial savings and decreasing of processing times [1].

The industrial application has certain disadvantages as low penetration of radiation in bulk products, low absorption of incident energy depending on the dielectric properties of materials and, finally, the uneven heating that occurs in foods with certain geometries and sizes as well as in foods which dielectric properties drastically change with temperature [2,3]. There is a similar problem with microwave thawing, due to preferential absorption of electromagnetic energy by liquid water compared to ice, caused by differences between dielectric properties ("runaway heating").

There is also experimental evidence that the shape and size of the product generates non-uniformity in internal temperature profiles during heating, particularly inside the cylinders and spheres and at the corners in parallelepiped shapes [4–8].

Several authors suggested some ways to reduce the intensity of non-uniformity in temperature profiles. Taher and Farid [9] and Gunasekaran and Yang [10] demonstrated the effectiveness of using power cycle during the microwave heating. As a disadvantage, the total process time is longer than under continuous power

* Corresponding author. 47 y 116, (B1900AJJ) La Plata, Buenos Aires, Argentina. Tel./fax: +54 221 4890741.
*E-mail address:* lacampa@ing.unlp.edu.ar (L.A. Campañone).

http://dx.doi.org/10.1016/j.applthermaleng.2014.08.048
1359-4311/

application. During microwave drying, Koné et al. [11] studied a drying strategy to improve the quality of dried products by using controlled power density. This technique is useful in drying process, where the mass of the product decreases strongly with the time and this provokes an increase of power absorption.

Geedipalli et al. [12] studied the role of a carousel in improving even heating of food in a microwave oven. They determined that the carousel helps in increasing the temperature uniformity of the food by about 40%. Another frequently used alternative is the movement of the material during the heating (use of fluidized beds, spouted bed dryers, rotary chambers, conveyor belts, etc.) [13].

Jet impingement (JI) is another method that was related to microwaves, giving rise to hybrid ovens [14,15]. In JI ovens, air can remove the water located at the surface of the food. At the same time, these ovens easily produce surface browning, needed in baked foods.

The variable-frequency technique is one of the most effective methods for improving field uniformity inside the resonant cavity. Conventional fixed-frequency microwave heating often results in localized heating as a result of local spatial fluctuations in the electromagnetic fields that cause non-uniform distribution within microwave cavities, thus leading to uneven heating and potentially poor product quality [16]. This technique works by sweeping through a band width of frequencies which are cycled through consecutively and launched into the cavity, resulting in different standing waves with many resonant modes. By sweeping through different frequencies, several possible cavity modes are excited, corresponding to different distributions of hot spots within the cavity. Then, these overlapped resonance modes result in a time-averaged uniformity. However, the geometry of the product should be taken into account: certain geometries, like spheres and cylinders usually cause maximum values at the center and the dielectric properties change due to the frequency dependence [17].

Nevertheless, the behavior of foods heating can be altered by working at a fixed frequency, knowing and technologically applying the resonance phenomenon inside the product in order to achieve more even temperature profiles.

The resonances are defined as values of maximum power absorption due to the interaction of the incident waves through transmitted and reflected waves within the material. For its application, the study of external behavior of the product should be complemented by the knowledge of internal behavior as well. This requires to control the pattern in the cavity and to characterize the profiles developed inside the product.

Resonances due to uniform plane waves were extensively studied by Bhattacharya and Basak, early in one dimensional samples [18,19]; therefore, for composite systems, like foods and ceramic plates [20–24]; they observed the resonance phenomena by the analysis of the individual traveling waves inside the sample, the transmitted and reflected waves, and their interactions. They established the position of maximum absorption points inside the sample, it occurs when the phase angle of transmitted wave coincides with the reflected one. Finally, their analysis permits to follow some useful strategies for optimal commercial processing.

In the present paper, we evaluate from the experimental and theoretical standpoints the controlled heating of foods, by changing the phases of two opposite electric field excitations and their interaction within food samples during thermal processing.

The purpose of this paper is to demonstrate the favorable effects of this electric fields phase change on the uniform heating of food. This work is an extension from a previous work [8].

Current work attempts to analyze the resonances by predicting the electromagnetic energy distribution outside and its value inside the foods through the solution of Maxwell equations. With this aim, we present a 3D mathematical model in order to solve the energy transfer during the microwave heating process. The analysis is focused into the product–radiation interaction, considering the dielectric properties of the product as temperature dependent. The numerical predictions allow us the study of the controlled microwave heating through the resonance phenomenon and to develop strategically internal patterns of heating by altering the phases of the incident waves, which achieve greater uniformity of the final temperature profiles.

## 2. Materials and methods

### 2.1. Experimental design

The aim of this work is to experiment with incident wave interference; according to this, the experimental procedure consisted in the heating of samples submitted to two incident waves impacting over both faces of the testing material.

An experimental oven with a 500 W magnetron oscillator was built (Fig. 1) to conduct food heating tests in a controlled way and coupled to a nonstandard waveguides system (80 × 32 mm) where the electromagnetic wave is conducted in the $TE_{10}$ dominant mode with work frequency of 2.45 GHz. The design includes a microwave power generator, from which the signal is split into two equal and coherent wave fronts through a power splitter in waveguide and both signals are conducted through the elbows to a straight waveguide section where the testing sample can be introduced. The power splitter was built in order to be adapted to minimize reflections towards the microwave generating source, which may cause damage.

During the experiments, the average temperature increase after an exposure time (30 s) and the temperature history at a fixed position inside the sample were measured. The initial (room temperature) and final temperatures were recorded by T-type thermocouples connected to a data acquisition system. Besides, the temperature inside the samples was measured using an optical temperature sensor model FOT-L (Fiso Techno. Inc, Canada). The optical fiber probe worked in a rank from −40 °C to 300 °C with an accuracy of ± 1 °C. The probe was introduced inside the product from the upper wall of the waveguide, to record the material temperature during the heating experiments. The thermal histories were used to validate the proposed mathematical model.

The samples were contained in trays made of acrylic (material transparent to the radiation) with three sizes 80 × 32 × 100 mm (tray A), 80 × 32 × 50 mm (tray B) and 80 × 32 × 25 mm (tray C) (Fig. 2a). Preliminarily, trays were placed inside the waveguide. The straight section of the guide has a removable window through which the samples can be inserted; thus the electromagnetic waves may come into contact with both faces (Fig. 2b). In all cases, samples covered all the waveguide width and height, only varying their thickness.

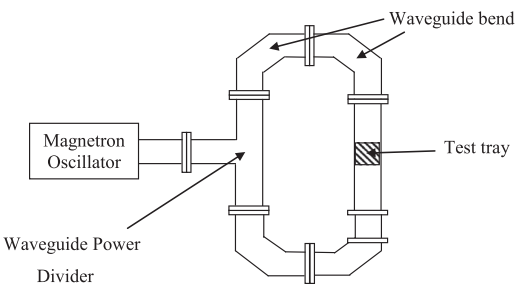


**Fig. 1.** Equipment top view diagram.

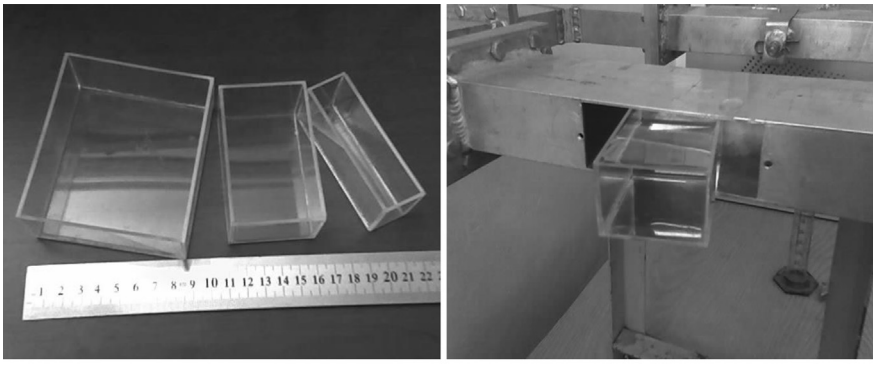

(a) (b)

**Fig. 2.** a) Test trays used in the experiments; b) Window made in the equipment for the input of the samples.

Test trays were filled up with water or mashed potatoes made from dehydrated powder that was rehydrated with a relation of 250 g mashed potatoes/1500 mL water. In Table 1, thermal and dielectric properties of tested materials are specified.

### 2.2. Mathematical model

#### 2.2.1. Electromagnetic field

A mathematical model was developed to predict the electromagnetic field distribution inside the waveguide and the trays containing the material in 3D domain (Fig. 3).

For this purpose, Maxwell's equations were solved with the following assumptions:

- Electromagnetic field outside the samples presents $TE_{10}$ mode.
- The absorption of microwave by air in a rectangular waveguide is negligible.
- The walls of rectangular waveguide are considered perfect conductors.
- The ends of the waveguide are configured as ports, each one having a phase $\theta_1 - \theta_2$.

To calculate the spatial distribution of the electric field, Eq. (1), derived from Maxwell–Ampere equations, is solved in both subdomains (air and tray).

$$\nabla \times \mu_r^{-1}\left(\nabla \times E\right) - k_o^2 \varepsilon_{rc} E = 0 \tag{1}$$

being

$$\varepsilon_{rc} = \varepsilon' - i\varepsilon'' \tag{2}$$

**Table 1**
Thermal and dielectric properties of materials.

| Property | Water | Mashed potatoes |
|---|---|---|
| $k$ Thermal conductivity [W/(m K)] | 0.5[a] | 0.45[c] |
| $\rho$ Density [kg/m$^3$] | 1000[a] | 1050[c] |
| $C_p$ Specific heat [J/(kg K)] | 4184[a] | 3640[c] |
| $\varepsilon'$ Dielectric constant (dimensionless) | $88.15 - 0.414T + 0.313\cdot10^{-2}\,T^2 - 0.046\cdot10^{-4}\,T^3$[b] | $0.209T + 73.7$[d] |
| $\varepsilon''$ Dielectric loss factor (dimensionless) | $\varepsilon'(0.323 - 9.5\cdot10^{-3}\,T + 1.27\cdot10^{-4}\,T^2 - 6.13\cdot10^{-7}\,T^3)$[b] | $0.07T + 17.7$[d] |

[a] [25].
[b] [26].
[c] [27].
[d] [28].

where $\varepsilon_{rc}$ is the complex relative electrical permittivity which consists of two parts: a real component $\varepsilon'$ that represents the ability of the material to store energy and an imaginary part and $\varepsilon''$ that accounts for the capacity to dissipate energy, $\mu_r$ is the relative magnetic permeability and $k_o$, the propagation constant, defined as:

$$k_o = \alpha + i\beta \tag{3}$$

$$\alpha = \frac{2\pi f}{c}\sqrt{\frac{\varepsilon'\left(\sqrt{(1+\tan^2\delta)}+1\right)}{2}} \tag{4}$$

$$\beta = \frac{2\pi f}{c}\sqrt{\frac{\varepsilon'\left(\sqrt{(1+\tan^2\delta)}-1\right)}{2}} \tag{5}$$

where $f$ is the frequency of radiation and the loss tangent ($\tan\delta$) is calculated using the dielectric properties of the food material:

$$\tan\delta = \frac{\varepsilon''}{\varepsilon'} \tag{6}$$

Boundary conditions for $TE_{10}$ mode can be formulated as follows:

For the outer waveguide boundary, the condition of perfectly conducting boundary was chosen, that is:

$$E_t = 0 \quad H_n = 0 \tag{7}$$

where the subscript $t$ denotes the tangential and $n$ the normal direction, respectively.

At the air-test tray interfaces, continuity conditions were considered.

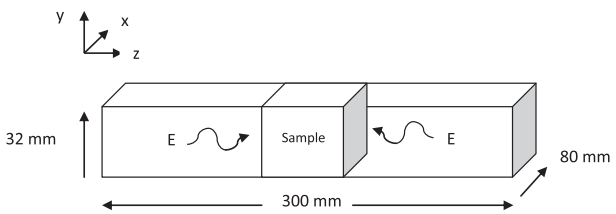


**Fig. 3.** Schematic diagram of the control volume: the straight waveguide with the inserted tray.

$$E_{t,1} = E_{t,2} \quad H_{t,1} = H_{t,2} \tag{8}$$

where the subscript 1 indicates air and 2 the sample.

Regarding the guide ends, they are configured as ports.

#### 2.2.2. Temperature profiles

The microscopic energy balance was developed to predict temperature profiles during food heating by microwaves; the following assumptions were done:

- Uniform initial food temperature.
- Temperature-dependent dielectric properties.
- Regular 3D geometry.

The microscopic energy balance which describes food thermal behavior, regarding its interaction with microwaves, is the following [23]:

$$\rho C_p \frac{\partial T}{\partial t} = \nabla(k\nabla T) + Q \tag{9}$$

where $\rho$ is the sample density, $C_p$ is the thermal capacity, $k$ is the thermal conductivity, $T$ is the temperature and $Q$ is the heat source, generated by the interaction sample-MW.

The energy balance (Eq. (9)) was solved taking into account heat conduction mechanism at air/sample interface represented by the following boundary condition:

$$-n_1 \cdot q_1 - n_2 \cdot q_2 = 0 \tag{10}$$

where $n$ is the normal vector to the surface of the sample, $q$ is the heat flux; the subscript 1 indicates air and 2 the sample. Besides, isolation condition was considered for the waveguide walls.

The microscopic energy balance is solved by knowing the volumetric energy source $Q$, depending on the distribution of the electric field, the frequency of the radiation and the properties of the material [24]:

$$Q = \frac{1}{2}\omega\varepsilon_0\varepsilon'' E.E^* \tag{11}$$

where $E^*$ is the complex conjugate electric field.

Coupled electromagnetic and energy Eqs. (1) and (9) with their initial and boundary conditions were solved by the numerical technique of Finite Elements Method, using the commercial software COMSOL Multiphysics (version 3.4, USA).

COMSOL Multiphysics TM software utilizes a partition into simpler forms of the geometric model (mesh), for the application of the numerical method. The amount of elements (or refinement) of the used mesh could influence on the model representation. Table 2 shows the mesh parameters used for two samples.

Harmonic propagation analysis was considered to solve Eq. (1) while the microscopic energy balance Eq. (9) was solved by the transient model using the direct solver UMFPACK.

The calculations took a few seconds with the direct solver to reach the final time of the process. COMSOL software estimates the values of electric field at each food position, the energy density delivered to the food (Eq. (11)) and is able to predict temperature profiles at each time step. From the numerical predictions, non-uniformity (NU) of temperature profiles was calculated as a standard deviation with respect to the average temperature [8].

**Table 2**
Mesh parameters used in the numerical simulation.

| Mesh parameters | 2.5 cm Thickness | 10 cm Thickness |
|---|---|---|
| Mesh points | 567 | 1996 |
| Tetrahedral elements | 2199 | 8426 |
| Boundary elements | 734 | 1804 |
| Side elements | 130 | 167 |

## 3. Results and discussion

### 3.1. Use of the mathematical model for simulating experimental data

The developed mathematical model was used for the prediction of temperature profiles. The numerical predictions were contrasted against experimental temperature data obtained in our laboratory. Firstly, the trays were filled with water. Water was selected because is the major component in fresh foods. Trials consisted in heating over a 30 s period.

Predicted and experimental values of volumetric mean temperature increase for water are shown in Table 3. It can be observed the proposed model is successful in the prediction of the mean temperature increase in liquid samples, being water representative of this type of products. It is observed that as the sample size decreases, the temperature increase is larger at equal heating times. As can be seen below, it could be attributed to the resonance phenomenon, which provokes an increase in heating rate.

Moreover, the possibility of predicting local temperature in function of time in another material (semisolid sample) was evaluated. Reconstituted mashed potatoes were chosen because they easily allow the optical sensor to be introduced into the tray. Predicted values were compared to the experimental ones obtained in sample size B which was completely filled with material. Temperature at the geometric center was determined. Evolution of predicted temperatures at this point and values obtained experimentally are shown in Fig. 4.

In the two proposed experiments, the model employs temperature dependent dielectric properties; therefore, balance Eqs. (1) and (9) are strongly coupled. From the comparison in Fig. 4, it is observed that the model accurately predicts the thermal history of the analyzed sample.

From these results it may be observed that the proposed model is adequate and properly predicts the mean temperature of liquid samples and furthermore is also able to reproduce the thermal history of a point inside of a semi-solid material, by being sensitive to the change in dielectric properties.

Therefore, the proposed model was used to analyze the electromagnetic and thermal behavior inside the system and to select the optimal conditions of heating in order to achieve uniformity at the final profiles.

### 3.2. Numerical predictions of the mathematical model

Firstly, the mathematical model was used to predict electric field distribution in the empty straight waveguide section with microwaves traveling in opposite directions, fed in phase ($\theta_1 = \theta_2$). Predicted results are shown in Fig. 5. It can be observed that the electromagnetic fields interaction from both ends of the guide

**Table 3**
Experimental and numerical predictions of temperature increase in water samples.

| Sample trays | Heating time (s) | Number of samples | Experimental average temperature increase (°C) | Numerical average temperature increase (°C) |
|---|---|---|---|---|
| A | 30 | 15 | 2.4 | 2.4 |
| B | 30 | 10 | 2.8 | 2.9 |
| C | 30 | 10 | 6.9 | 6.9 |

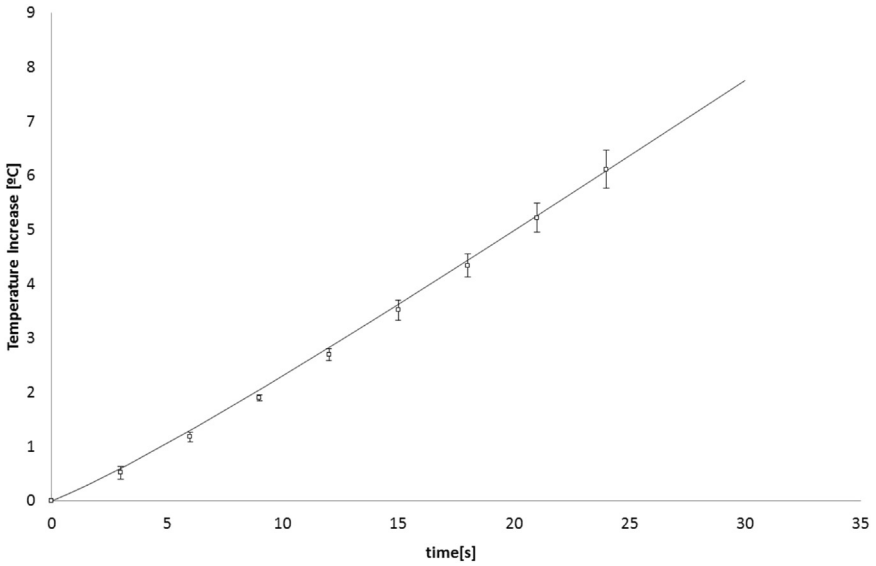


**Fig. 4.** Predicted thermal history (continuous line) and experimental values (symbols) obtained at the center of the tray B (mashed potatoes).

causes a standing wave with maximum and minimum values in fixed positions inside the waveguide. Constructive interference (CI) occurs when the angle difference between the traveling waves is null. Due to CI between the waves, four maximum values appear inside the straight waveguide. The maximum value of electric field intensity is around $3 \cdot 10^4$ V/m. Besides, the destructive interference is shown through the three minimum values, one of them located at the center, $z = 150$ mm.

In order to predict the effect of including the test tray into developed profiles, the prediction software (with the working conditions of Fig. 5) was modified as to simulate the existence of trays of different sizes. The insertion of blocks inside the waveguide simulates, in its central section, the different trays employed in the experiments. At this stage, the electromagnetic and thermal models are solved. The results are presented according to the size of the sample. In this work, the numerical study was carried out for the three sample sizes (thicknesses) used in the experimental design: 10, 5 and 2.5 cm (trays A, B and C, respectively).

The predicted results of inserting test tray A (10 cm thickness) - from the electromagnetic and thermal points of view – may be observed in Fig. 6 (views *x-z*).

Fig. 6a and b show the material response with regard to the electric field and temperature profile considering the waves were fed in phase. It can be observed the change in electromagnetic patterns outside the sample with respect to the empty guide (Fig. 5). When the waveguide is empty, the incident waves pass through the cavity having low permittivity and loss factor. Then, when the sample is present, the waves interact with a product having high values of these properties, a portion of incident wave is reflected and resonated, while other is transmitted. Besides, there is

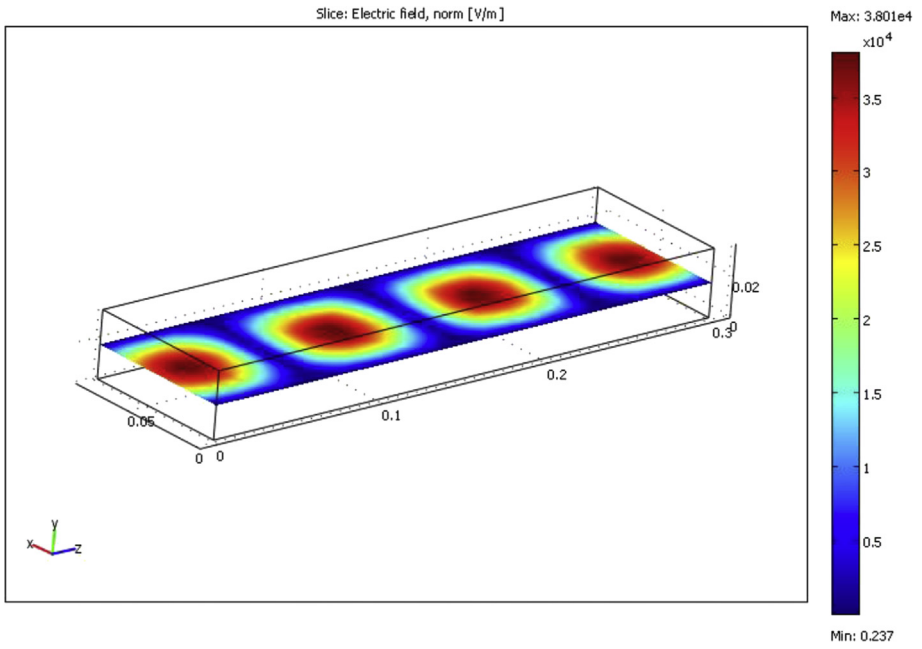


**Fig. 5.** Predicted distribution of the electric fields ($E_1$, $E_2$) inside the waveguide (traveling in opposite directions, in phase).

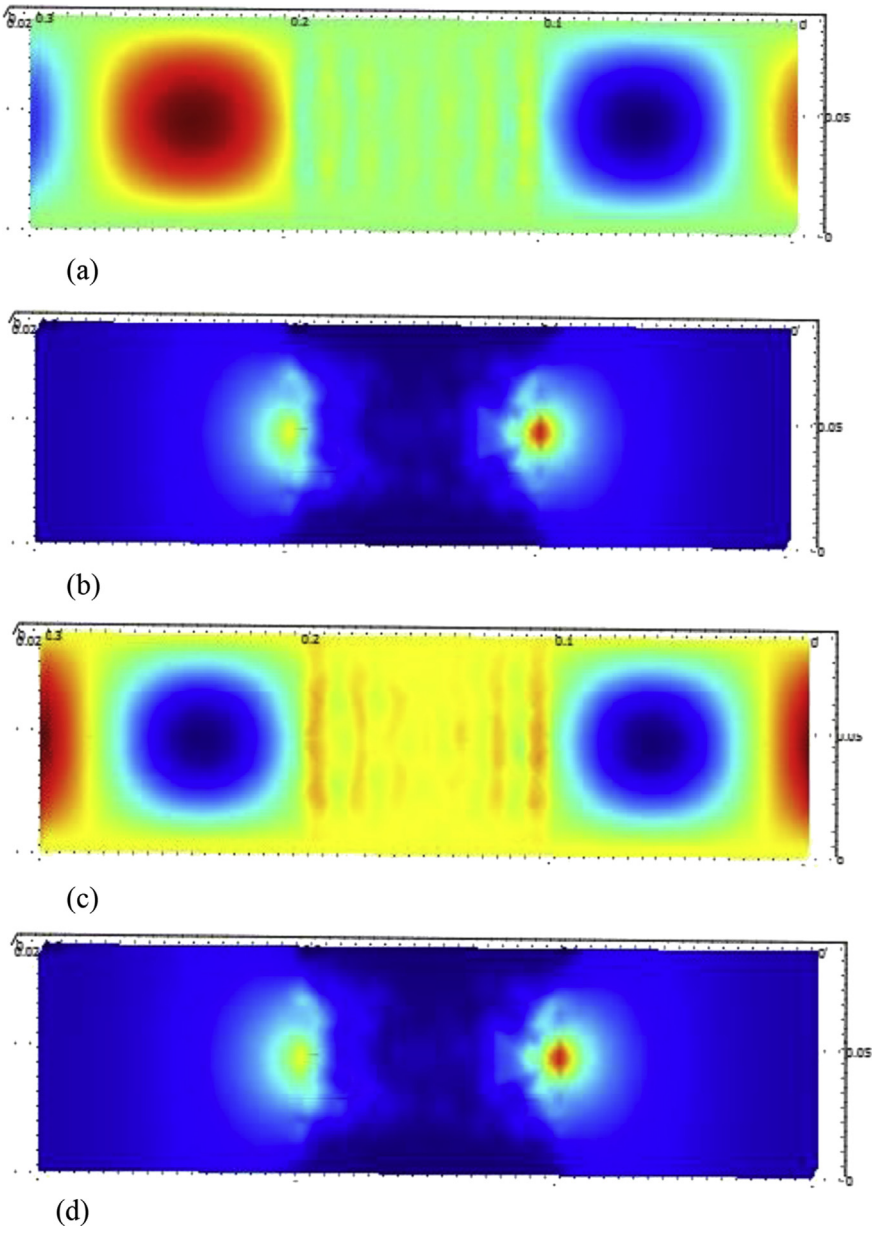


**Fig. 6.** Predictions of the proposed model in electromagnetic-thermal terms for test tray A (size 10 cm), filled with mashed potatoes: a) and b) waves in phase; c) and d) waves in antiphase (Incident power in both faces = 150 W, *T* initial = 303 K).

an inversion of the electric field direction, mainly due to reflections caused by the impact faces of the test tray.

The numerical solution of the electromagnetic field (Eq. (1)) gives more evident results in terms of amount of points of maximum absorption of microwave power. Although two points of maximal absorption are located at the ends of the sample, six low intensity inner points appeared (Fig. 6a). The temperature values do not show a strong oscillatory behavior only two hot spots can be observed (Fig. 6b). The resonance phenomenon is not dominant in samples of this size, and the internal waves overlapping do not generate pronounced hot spots within the sample. These results are consistent with those reported by other authors on wet food samples of this size [7].

Fig. 6c and d show the distribution of electric field and temperature developed when the waves were fed in antiphase way. From the numerical results it is observed that the electric field distribution within the product is not very sensitive to the phase changes of the incident waves, although the smooth inner points change their amount and position. Predicted maximal temperature of the test tube ($T_{max}$) was 24 °C (Fig. 6a and c), the maximum values of electric field intensity ($E_{max}$) inside the sample were 2360 V/m and 2297 V/m (Fig. 6b and d) on the faces exposed to radiation. Besides, this sample size shows 3.2 °C of non uniformity (NU) in temperature profiles (phase and antiphase operation). It is interesting to remark the reduction of the intensity of the external electric field, in the empty waveguide the high value was $3\,10^4$ V/m, while this value decreased to 5134 V/m and 5093 V/m (phase and antiphase operation). This reduction occurs due to the absorption and reflection of the incident waves in the air/sample interfaces.

The same numerical analysis was performed for smaller size samples. Fig. 7 presents the results obtained for a sample of 5 cm thickness (tray B). In these numerical results it may be observed that this test tray is more sensitive to the changes of external electric field. When the sample is exposed to the incident waves in

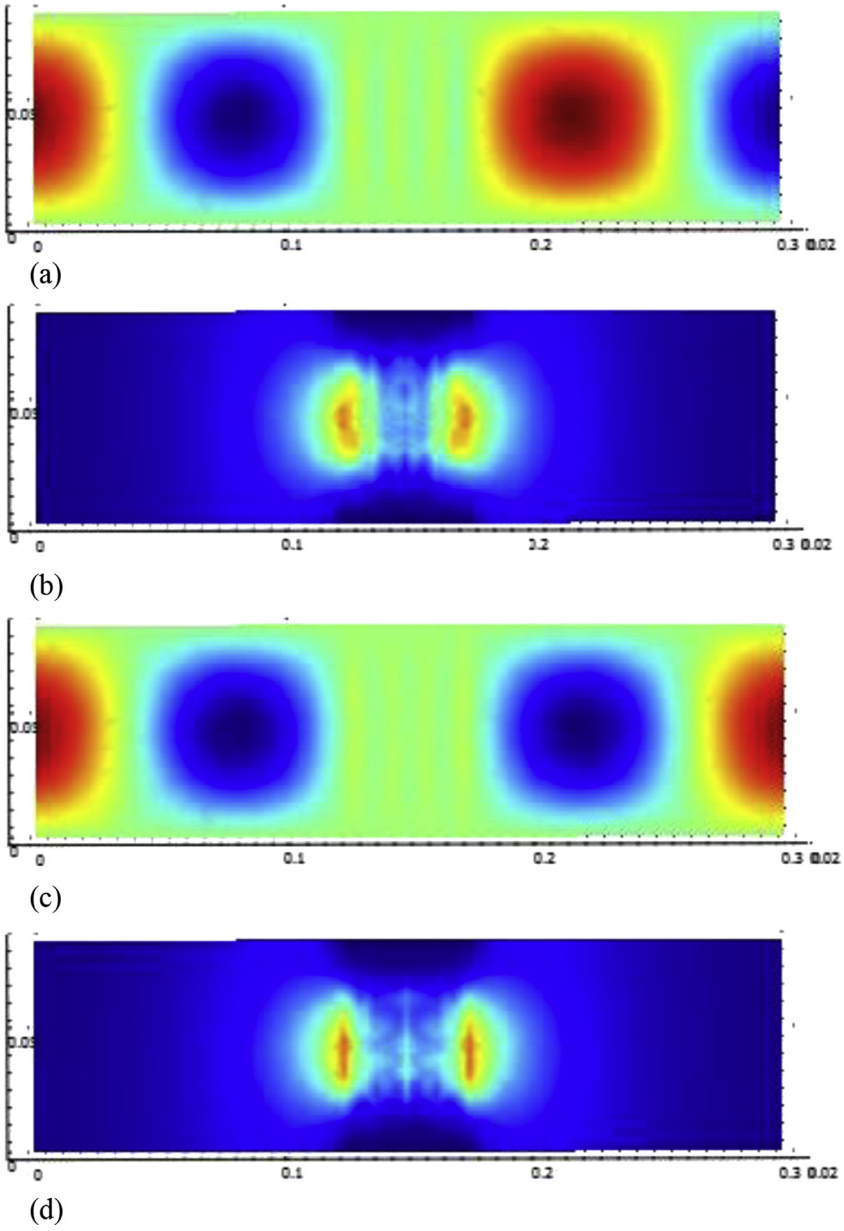


**Fig. 7.** Predicted electric field distribution and temperature profiles during heating of mashed potatoes, (tray B, size 5 cm) with input signals to the straight guide section in phase (a–b) and antiphase (c–d).

phase, three inner hot spots appear (Fig. 7a); particularly, the center becomes a hot spot concentrating energy (Fig. 7b). Maximum predicted of temperature increase of the test tray was 17 °C, at the ends of the tray. The value of the intensity at this zone was 1881 V/m and the NU parameter was 3.33 °C.

The change of phase in incident waves fed into the straight guide section ($\theta_1 - \theta_2 = \pi$) generates a change in the amount of these spots and causes a shift on the position of hot spots (Fig. 7c and d). In this kind of operation the central zone becomes a cold spot, but symmetrical four inner hot points provoke a temperature increase of 20 °C (at the faces exposed to radiation). The value of the electric field in this region was about 840 V/m and the value of NU was 4.6 °C.

The resonance phenomenon is more relevant in this size of product (in phase and antiphase operation). The decrease in the absorption of electromagnetic energy, due to destructive interference of the waves inside the sample, provokes a decrease in temperature values at the same input power into the waveguide, in comparison with 10 cm thickness.

Finally, the analysis was carried out for tray C (sample size 2.5 cm). For smaller samples the results are shown with discrete phase shifts of $\pi/4$ ($\theta_1 - \theta_2$). Table 4 shows the maximum values of the incident electric field at left ($E_{max,l}$) and right ($E_{max,r}$) faces of the sample, the maximum value of temperature increase ($T_{max}$) and NU for each phase shift.

The numerical results obtained on this size put the resonance phenomenon in relevance. Fig. 8a and b show the electromagnetic and temperature profiles when the sample is irradiated with the waves in phase. A symmetrical and uneven distribution can be observed, the ends of the tray and two inner points become hot spots (smoother), and the centre zone becomes cold (NU = 11.4 °C).

The phase shift between the incident waves in $\pi/4$ alters external electromagnetic patterns, causing a clear response within

**Table 4**
Numerical predictions of the incident electric field at left ($E_{max,l}$) and right ($E_{max,r}$) external faces of the sample, the maximum value of temperature increase ($T_{max}$) during 30 s of heating and non-uniformity parameter (NU) for each phase shift.

| Phase shift $\theta_1 - \theta_2$ (rad) | $E_{max,l}$ (V/m) | $E_{max,r}$ (V/m) | $T_{max}$ (°C) | NU (°C) |
|---|---|---|---|---|
| 0 | $1.7 \cdot 10^4$ | $1.7 \cdot 10^4$ | 54.0 | 11.4 |
| $\pi/4$ | $1.7 \cdot 10^4$ | $1.4 \cdot 10^4$ | 47.7 | 10.0 |
| $\pi/2$ | $1.7 \cdot 10^4$ | $2.2 \cdot 10^4$ | 33.0 | 6.9 |
| $3\pi/4$ | $1.8 \cdot 10^4$ | $1.2 \cdot 10^4$ | 23.4 | 4.3 |
| $\pi$ | $2.0 \cdot 10^4$ | $2.0 \cdot 10^4$ | 15.8 | 3.4 |

the sample. The overlapping of main incident waves with internal reflections generates a rapid movement of the hot zone to the left wall of the sample. This is due to the imposed external pattern; a shift of $\pi/4$ generates a field weakening in one of the faces (Fig. 8c) and the opposite face changes into a hot spot (Fig. 8d). Non uniform electromagnetic and temperature profiles dominate the pattern in this kind of operation (NU = 10 °C).

This behavior is more intense on $\pi/2$ phase lag (Fig. 8e and f). An inversion of the external electric field direction occurs in the right zone of the sample. The temperature profile exhibits a strong absorption at the left zone and poor at the opposite wall, following the electromagnetic profile (see Table 4).

When the phase shift is $3/4\pi$ the external wave pattern changes again. The inner electric field tends to have a symmetrical shape (Fig. 8g). The hot zone (left side) moves towards the central region, causing a displacement to the opposite face (Fig. 8h).

Finally, a phase lag of $\pi$ in the incident waves establishes a symmetrical electromagnetic and thermal pattern. The central region becomes a hot zone. Supply waves in antiphase way causes a minimum NU and temperature increase values (Table 4).

From the obtained numerical results, sample C exhibits a strong resonant behavior. It could be explained considering the constructive interference theory. In 1D analysis, it is demonstrated this occurs for certain product sizes, where the interference between incident waves and the first reflection will be constructive at $2L/\lambda_m = n$, being $\lambda_m$ the wavelength in the medium, for samples with both sides exposed to microwaves [29]. If we consider the wavelength of water radiation as 1.4 cm (at room temperature), tray C shows a resonant behavior causing extra maximum energy absorption.

The observed phenomenon is a specific characteristic in microwave heating that cannot be observed in traditional convective heating [8]; the developed mathematical model based on the solution of Maxwell's equations allows predicting the appearance of such resonances for these product sizes.

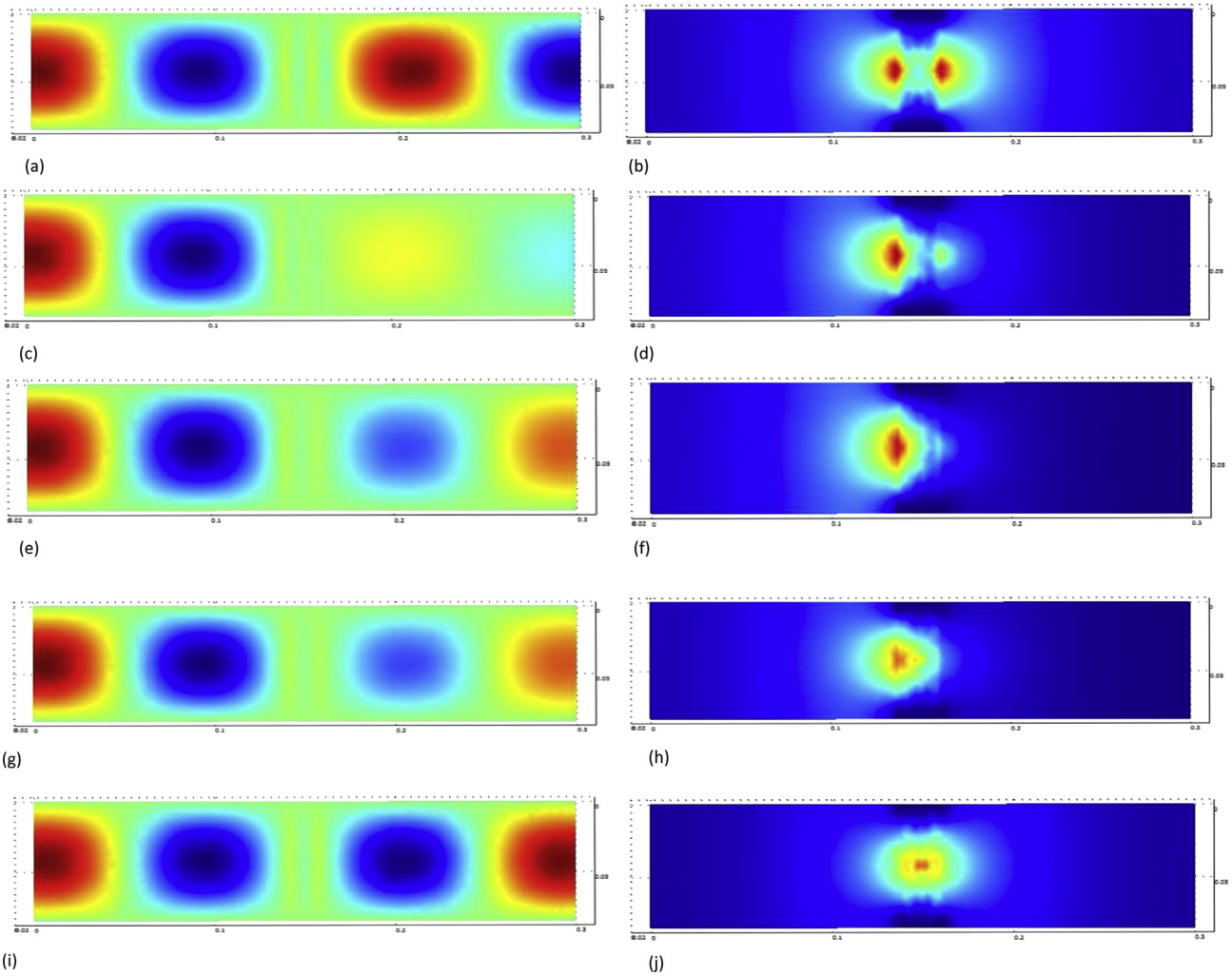


**Fig. 8.** Predicted electric field distribution and temperature profiles during heating of mashed potatoes, (tray C, size 2.5 cm) with discrete phase shifts of $\pi/4$ on signals of entrance to the straight guide section.

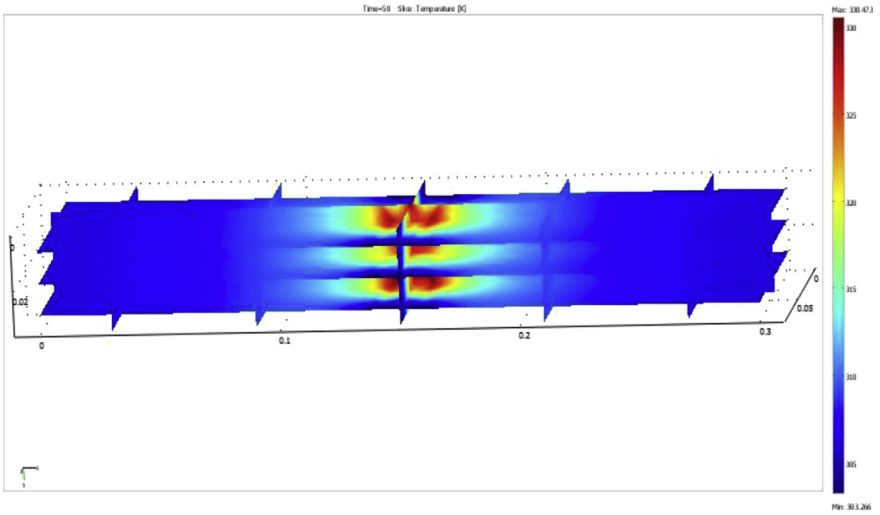

**Fig. 9.** Temperature profile obtained working 10 s in phase and 50 s in antiphase (size 2.5 cm).

### 3.3. Strategies to achieve uniformity

Microwave heating simulation was carried out on a specific sample thickness selected based on greater power distribution within the sample (tray C). The strategy used was the interference of the incident electromagnetic waves (IEW) to produce changes in the developed temperature profiles. When radiation is applied "in phase", peaks and valleys appear inside the food (as shown in previous sections) during a time period. By changing the phase of one incident wave respect to the other, the hot and cold spots change their position during the time needed to complete the operation; this in turn can improve the temperature uniformity.

The software was applied to simulate the behavior of food heated according to this strategy. The incident waves were of the same intensity $P = 150$ W. The operation was carried out in phase during the first fixed heating period ($time_{phase}$) and with a shifted phase of $\pi$ ($time_{anti}$) to complete the process. The simulations were carried out at 5 different conditions:10 s $time_{phase}$/50 s $time_{anti}$, 20 s $time_{phase}$/40 s $time_{anti}$, 30 s $time_{phase}$/30 s $time_{anti}$, 40 s $time_{phase}$/20 s $time_{anti}$ and 50 s $time_{phase}$/10 s $time_{anti}$. A typical temperature profile is shown in Fig. 9. The most uniform final temperature profile in the entire volume of the material was obtained by applying this technique. Numerical results of this type of operation are presented in Fig. 10. It can also be observed that the condition 5 (50 s $time_{phase}$/10 s $time_{anti}$) gives advantage to temperature increase at the expense of a very non-uniform temperature profile.

The operation in phase during 60 s gives a value of 21 °C of NU and 77.76 °C of maximum value of temperature increase; in antiphase operation during 60 s the value of NU is 6 °C with 24 °C in temperature increase. The proposed operation ($time_{phase}$/$time_{anti}$) in all conditions gives intermediate values of NU parameter suggesting a more uniform temperature profiles (Fig. 10).

The most adequate heating strategy has to be selected according to the particular size and composition of sample, the desirable temperature increase and the allowed NU value for selected heating conditions. This procedure is currently under experimental study at our laboratory.

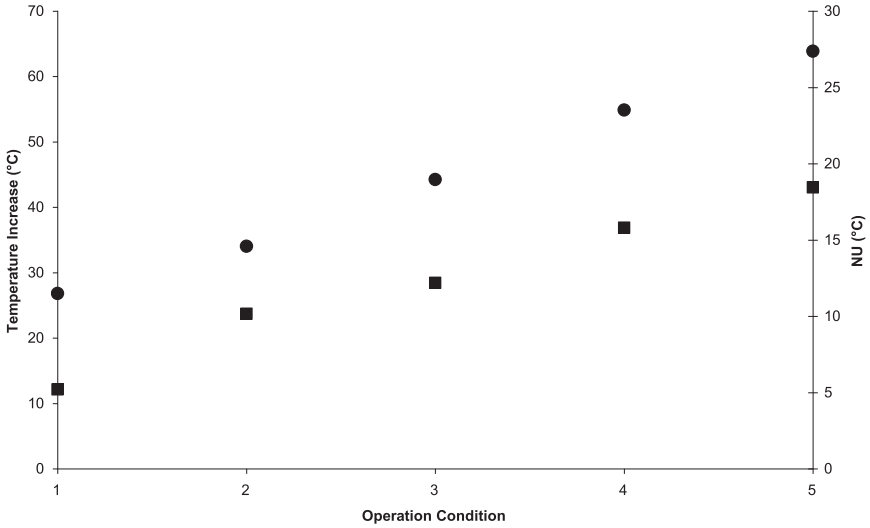


**Fig. 10.** Temperature increase (circles) and non uniformity parameter NU (squares) obtained in different operation conditions: 1) 10 s $time_{phase}$/50 s $time_{anti}$, 2) 20 s $time_{phase}$/40 s $time_{anti}$, 3) 30 s $time_{phase}$/30 s $time_{anti}$,4) 40 s $time_{phase}$/20 s $time_{anti}$, 5) 50 s $time_{phase}$/10 s $time_{anti}$.

## 4. Conclusions

In the present work, a 3D numerical analysis of the controlled heating of foods was done. The effect of the interference between the incident waves in electromagnetic and temperature profiles was made evident. In particular, smaller samples were more sensitive to the imposed changes of electromagnetic external pattern.

In the smallest analyzed sample, the change of incident electric field phases provokes a weakening of field intensity from one wave respect the other, while the electric fields change their direction. Sample responds to the imposed pattern showing maximum temperature values on the surface that – while phase change progresses – are moved to the center.

One strategy was selected to reduce uneven temperature profiles: the application of the waves in phase during a first period and in an antiphase way during the rest of the heating time. The predicted results suggest that the application of this practice could be effective when selecting a combination of convenient times in phase and counter phase operation. It needs a previous analysis of the product resonance, which strongly depends on the size and dielectric properties of the material.

## Acknowledgements

The authors gratefully acknowledge the financial support provided by Universidad de La Plata; ANPCyT (PICT 2518-2010) and Consejo Nacional de Investigaciones Científicas y Técnicas (CONICET) of Argentina.

## References

[1] L.A. Campañone, N.E. Zaritzky, Mathematical analysis of microwave heating process, J. Food Eng. 69 (2005) 359–368.
[2] H.S. Ku, E. Siores, A. Taube, J.A.R. Ball, Productivity improvement through the use of industrial microwave technologies, Comput. Indus. Eng. 42 (2002) 281–290.
[3] S. Farag, A. Sobhy, C. Akyel, J. Doucet, Temperature profile prediction within selected materials heated by microwaves at 2.45 GHz, Appl. Therm. Eng. 36 (2012) 360–369.
[4] M.E.C. Oliveira, A.S. Franca, Microwave heating of foodstuffs, J. Food Eng. 53 (2002) 347–359.
[5] T. Basak, K.G. Ayappa, Role of length scales on microwave thawing dynamics in 2D cylinders, Int. J. Heat Mass Transf. 45 (2002) 4543–4559.
[6] T. Basak, Analysis of resonances during microwave thawing of slabs, Int. J. Heat Mass Transf. 46 (2003) 4279–4301.
[7] T. Basak, S.S. Kumaran, A generalized analysis on material invariant characteristics for microwave heating of slabs, Chem. Eng. Sci. 60 (2005) 5480–5498.
[8] L.A. Campañone, C.A. Paola, R.H. Mascheroni, Modeling and simulation of microwave heating of foods under different process schedules, Food Bioprocess Technol. 5 (2) (2012) 738–749.
[9] B.H. Taher, M.M. Farid, Cyclic microwave thawing of frozen meat: experimental and theoretical investigation, Chem. Eng. Process. 40 (4) (2001) 379–389.
[10] S. Gunasekaran, H. Yang, Effect of experimental parameters on temperature distribution during continuous and pulsed microwave heating, J. Food Eng. 78 (2007) 1452–1456.
[11] K.Y. Koné, C. Druon, E.Z. Gnimpieba, M. Delmotte, A. Duquenoy, J.C. Laguerre, Power density control in microwave assisted air drying to improve quality of food, J. Food Eng. 119 (2013) 750–757.
[12] S.S.R. Geedipalli, V. Rakesh, A.K. Datta, Modeling the heating uniformity contributed by a rotating turntable in microwave ovens, J. Food Eng. 82 (3) (2007) 359–368.
[13] Z. Li, G.S.V. Raghavan, V. Orsat, Temperature and power control in microwave drying, J. Food Eng. 97 (2010) 478–483.
[14] C.E. Walker, A. Li, Impingement oven technology-part III. Combining impingement with microwave (hybrid oven), Res. Dep. Tech. Bull. 15 (9) (1993) 1–6.
[15] A.K. Datta, R.C. Anantheswaran, Handbook of Microwave Technology for Food Applications, Marcel Dekker Inc., USA, 2005.
[16] C. Antonio, R.T. Deam, Comparison of linear and non linear sweep rate regimes in variable frequency microwave technique for uniform heating in materials processing, J. Mater. Process. Technol. 169 (2) (2005) 234–241.
[17] J.R. Bows, M.L. Patrick, R. Janes, A.C. Metaxas, D.C. Dibben, Microwave phase control heating, Int. J. Food Sci. Technol. 34 (1999) 295–304.
[18] M. Bhattacharya, T. Basak, New closed form analysis of resonances in microwave power for material processing, AIChE J. 52 (11) (2006) 3707–3721.
[19] M. Bhattacharya, T. Basak, A novel closed-form analysis on asymptotes and resonances of microwave power, Chem. Eng. Sci. 61 (19) (2006) 6273–6301.
[20] T. Basak, A.S. Priya, Role of metallic and ceramic supports on enhanced microwave heating processes, Chem. Eng. Sci. 60 (2005) 2661–2677.
[21] T. Basak, A.S. Priya, Role of ceramic supports on microwave heating of materials, J. Appl. Phys. 97 (8) (2005). Art. No. 083537.
[22] T. Basak, A. Meenakshi, A theoretical analysis on microwave heating of food slabs attached with ceramic plates: role of distributed microwave incidence, Food Res. Int. 39 (2006) 932–944.
[23] T. Basak, K. Aparna, A. Meenakshi, A.R. Balakrishnan, Effect of ceramic supports on microwave processing of porous food samples, Int. J. Heat Mass Transf. 49 (2006) 4325–4339.
[24] T. Basak, A. Meenakshi, Influence of ceramic supports on microwave heating for composite dielectric food slabs, AIChE J. 52 (2006) 1995–2007.
[25] N. Mohsenin, Thermal properties of Foods and Agricultural Materials, Gordon and Breach Science Publishers, London, 1980.
[26] W. Cha-Um, P. Rattanadecho, W. Pakdee, Experimental and numerical analysis of microwave heating of water and oil using a rectangular wave guide: influence of sample size, positions, and microwave power, Food Bioprocess Technol. (2009) 1–15.
[27] L. Zhou, V.M. Puri, R.C. Anantheswaran, G. Yeh, Finite element modelling of heat and mass transfer in food materials during microwave heating-model, development and validation, J. Food Eng. 25 (1995) 509–529.
[28] M. Regier, J. Housova, K. Hoke, Dielectric properties of mashed potatoes, Int. J. Food Prop. 4 (2001) 431–439.
[29] K.G. Ayappa, Modelling transport processes during microwave heating: a review, Rev. Chem. Eng. 13 (2) (1997) 1–67.